

## Geometric aspects of the ideal shear resistance in simple crystal lattices

V. V. BULATOV\*†, W. CAI‡, R. BARAN§ and K. KANG‡

†Lawrence Livermore National Laboratory, University of California,  
Livermore, CA 94550, USA

‡Department of Mechanical Engineering, Stanford University,  
Stanford, CA 94305-4040, USA

§Department of Mechanical Engineering, Rensselaer Polytechnic Institute,  
Troy, NY 12180, USA

(Received 20 October 2005; in final form 16 February 2006)

We present and analyze results of a large series of atomistic calculations of crystal resistance to shearing along rational planes of different orientations. The data computed for bcc and fcc crystals suggests that the interplanar spacing,  $d$ , is not a pertinent scaling parameter for the ideal shear resistance and that instead, plane orientation angle,  $\theta$ , is a more appropriate predictor of the resistance variations among crystal planes in the same crystallographic zone. By counting the interatomic bonds reaching across the shear plane, we obtain interpolation functions that accurately match the computed resistances in the whole range of plane orientations. Entirely defined by the lattice symmetries and geometry, the interpolation functions are universal for a given crystallographic class of materials. Within a given class, material specificity of the shear resistance is accounted for with just a few scaling parameters entering the interpolation functions.

### 1. Introduction

It is tempting to try to relate the shear strength of a crystalline material to its lattice geometry. As an indication that such a connection may exist, it is perhaps relevant to refer to vast empirical data revealing significant similarities in the yield behaviour of materials from the same crystallographic class [1]. The idea may also appear appealing because fundamentally, both the ground state crystal structure and its resistance to shear are defined by the detailed character of interatomic bonding. In his classic work published in 1926, Frenkel [2] derived his famous formula for theoretical shear stress,  $\sigma_{\text{th}}$ , required to overcome the lattice resistance to shearing along rational (crystallographic) planes

$$\sigma_{\text{th}} = \frac{\mu b}{2\pi d}, \quad (1)$$

---

\*Corresponding author. Email: bulatov1@llnl.gov

where  $\mu$  is the shear modulus,  $b$  is the lattice repeat vector (Burgers vector) and  $d$  is the spacing between two planes along which the sliding occurs. Largely confirmed as qualitatively accurate by the subsequent observations, Frenkel's relationship is frequently used in the textbooks and lectures in the discussions of the most basic aspects of crystal strength [3]. Perhaps a less appreciated fact is that Frenkel arrived at his remarkable formula before the principles of quantum mechanics were advanced and well before the nature of atomic bonding was clarified.

To motivate his mathematical treatment, Frenkel used a qualitative model in which resistance of a crystal to interplanar sliding is likened to friction between two saw-toothed surfaces or “files” I and II that remain interlocked in their normal, stress-free state. The basic query posed and answered by Frenkel was then “... how large the tangential force applied to file II has to be in order to make it slide over file I” [2]. Two additional arguments leading to the famous result were that (i) shear resistance must be a periodic function of shear displacement  $u$  with period  $b$  and that, (ii) in the limit of small  $u$ , the energy induced by shear must be related to the elastic shear modulus  $\mu$ .

Equation (1) has been influential in subsequent developments that led to further clarification on the nature of shear strength. Although only applicable to the ideal defect-free crystals, it has not only “survived” the eventual arrival and triumph of the dislocation theory but also contributed to the formulation of one of its cornerstones, the celebrated Peierls–Nabarro (PN) approach [4, 5]. In the latter, the resistance to dislocation motion comes in the form of periodic variations of the dislocation energy as a function of dislocation position in the glide plane. Starting from Frenkel's equation, equation (1), the effect of lattice geometry on shear resistance is further emphasized by the exponential dependence of the PN stress on the interplanar spacing  $d$ :

$$\sigma_p = \alpha\mu \exp\left(-\beta\frac{d}{b}\right), \quad (2)$$

where two dimensionless coefficients  $\alpha$  and  $\beta$  depend on the dislocation character. In the PN theory, the exponential dependence of the lattice resistance on the interplanar spacing  $d$  arises from a combination of two factors. Firstly, according to equation (1), the amplitude of the restoring stress is higher for the closely spaced crystal planes resulting in the higher Peierls stress. Secondly, the dependence on  $d$  is further amplified because the higher amplitude of the restoring stress leads to a narrower core. Just like equation (1), equation (2) is in general agreement with experimental observations showing that, as a rule, the dislocations glide on the most widely spaced crystallographic planes.

One of the reasons for recent renewal of interest in the topic is the newly acquired ability to compute the ideal shear resistance of a crystal using accurate atomistic approaches, including many-body interatomic potentials [6], tight binding [7] and density functional theory [8] methods. The ideas advanced by Frenkel [2] have been further developed by Vitek who proposed computation of the interplanar potential – subsequently referred to as the  $\gamma$ -surface or the generalized stacking fault (GSF) energy surface – atomistically, by making two halves of the crystal slide rigidly along

the glide plane [9]. The so-computed GSF surfaces were then used in numerous studies of dislocation core and mobility properties within the PN framework [10]. Another source of motivation for further studies is that the ideal shear resistance is not just a theoretical limit of shear strength but can be attained in certain experimental conditions, such as in metal whiskers and nano-wires or in nanoindentation experiments.

The purpose of this contribution is to report on the results of a large series of direct atomistic calculations in which the effect of crystal lattice geometry on the ideal shear resistance is systematically examined. The next section describes the methods used for computing the shear resistance. Section 3 then focuses on the results obtained for a bcc crystal and section 4 discusses similar data for two model fcc systems. Section 5 summarizes the findings.

## 2. Computational details

Most calculations to be discussed in the subsequent sections were performed using two interatomic potentials. Although both potentials have previously been shown to be reasonably accurate in describing various properties of molybdenum [11] and aluminium [12], it is not our purpose here to accurately compute the shear resistance in these two respective materials. Rather, our goal is to elucidate the qualitative relationship between the shearing resistance and the geometry of bcc and fcc lattices. Both potentials belong to the same general class of many-body embedded atom potentials. In the case of fcc crystal, we also performed a series of calculations using a pair-wise (6-12) Lennard-Jones potential function for comparison. Even though the very idea of ideal shear resistance is qualitatively simple, there exist several alternative measures that can be, and have been, used to quantify this concept. In the discussion that follows we will examine three such measures all expressed in the units of stress (figure 1). In method 1, we identify  $\sigma_{th}$  with the maximum slope of the two-dimensional GSF energy surface obtained by the rigid-block-sliding procedure, i.e. by computing the excess energy per unit area of the plane induced by sliding the halves along the selected plane by  $u$  without any relaxation of atomic positions. Method 2 is the same as the rigid-block-sliding but now allowing the spacing between two sliding half-crystals to relax to the minimum of energy for every value of the sliding displacement  $u$ . Finally, method 3 consists of applying and incrementing an appropriate (affine) shear strain on the crystal lattice and recording the value of the first maximum of shear stress induced in the crystal by such straining.

The measures of shear resistance were computed for multiple planes in the  $\langle 111 \rangle$  and  $\langle 110 \rangle$  zones for bcc and fcc systems, respectively. With one exception, we only considered displacement paths along the smallest repeat vector of each lattice, i.e. along  $\frac{1}{2}\langle 111 \rangle$  for bcc and along  $\frac{1}{2}\langle 110 \rangle$  for fcc. The only exception was that, for the fcc crystal, we also obtained  $\sigma_{th}$  for the  $\langle 112 \rangle$  direction on the  $\{111\}$  plane.

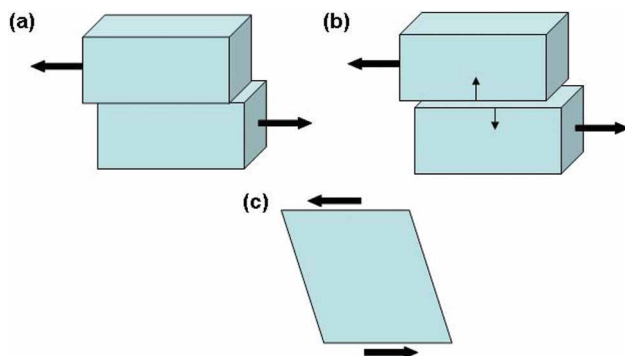


Figure 1. Three methods used for computing the ideal shear resistance. (a) The rigid-block-sliding method (method 1) where the upper half of the crystal slides on top of the lower half along a pre-selected crystal plane. (b) Method 2 is the same as method 1 except that, in addition to sliding along the plane, the upper half of the crystal is allowed to move vertically, away from the lower half, to attain a minimum energy. (c) Method 3 is the uniform (affine) straining of the crystal in the direction of shear along the plane.

### 3. Results and discussion – bcc crystal

Here we examine the resistance to sliding along the  $[111]$  direction in different planes of the  $[111]$  zone. Figure 2 shows  $\sigma_{th}$  computed by rigid-block-sliding, or method 1, plotted against the interplanar spacing  $d$  for 15 different planes. Also plotted for comparison is the  $1/d$  function drawn through the data point corresponding to the  $(\bar{1}10)$  plane with the largest  $d$ . The computed data suggests that the expected  $1/d$  dependence does not hold for this particular model of bcc molybdenum. To check whether this disagreement results from our use of method 1, we repeated some of the calculations using method 2 (block-sliding with vertical relaxation) and method 3 (uniform straining). The corresponding data points are also plotted in figure 2. Clearly, all three sets of computed data points show very similar variations confirming that plane spacing  $d$  is not a good scaling parameter for our model bcc crystal. At the same time, one particular subset of the data points (connected by the dashed line in the figure) appears to vary systematically as a function of  $d$ : this subset is formed by planes vicinal to the  $(\bar{1}10)$  plane in the sense illustrated in the inset in figure 2. Each plane in this subset was constructed so that the direction of the line tracing the plane edge,  $\mathbf{l}$ , referred to hereafter as the plane edge vector (PEV), is a combination of the PEV for plane  $(\bar{1}10)$  and the PEV for plane  $(01\bar{1})$ , i.e.

$$\mathbf{l}_n = \frac{1}{2}[11\bar{2}]n + \frac{1}{2}[2\bar{1}\bar{1}].$$

The Miller indices for the planes from this subset are  $(-n, n+1, -1)$ . More generally, any plane  $(n, m)$  of the  $[111]$  zone can be defined through its PEV vector  $\mathbf{l}_{nm}$  as

$$\mathbf{l}_{nm} = \frac{1}{2}[11\bar{2}]n + \frac{1}{2}[2\bar{1}\bar{1}]m.$$

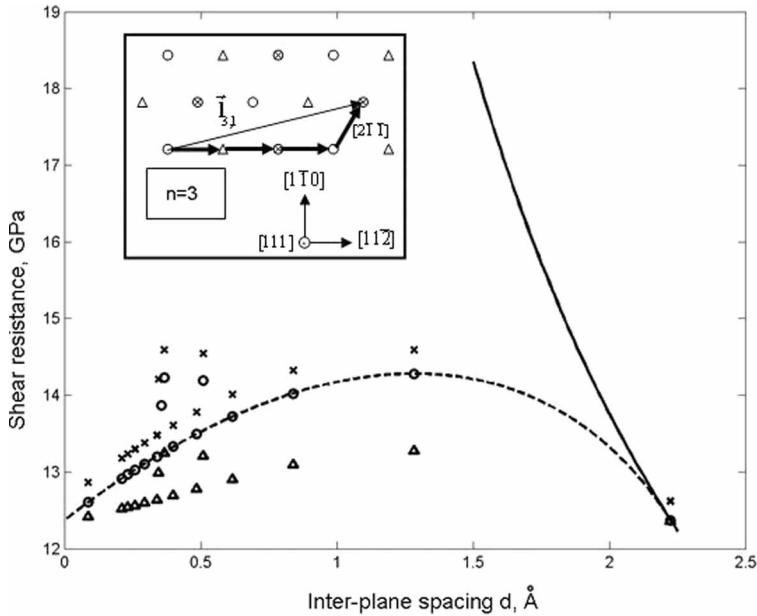


Figure 2. Shear resistances computed for the Finnis–Sinclair model of bcc molybdenum by method 1 (open circles), method 2 (crosses) and method 3 (triangles). In the latter case, only the data obtained for the twinning sense of shear is included. The solid line is the Frenkel’s equation with parameters selected to match the computed resistance for the most widely spaced {110} plane (farthest to right). The dashed curve is equation (3) obtained from the bond counting argument explained in the text. The inset shows the construction of the subset of planes vicinal to the horizontal “terrace”. Each plane in the subset is labelled by indices  $n$  and  $m$  equal to the numbers of times the horizontal and the inclined basis vectors  $[11\bar{2}]$  and  $[2\bar{1}\bar{1}]$  are taken to form the plane edge vector  $\mathbf{l}_{nm}$ : the case shown in the inset corresponds to  $n=3$  and  $m=1$ .

A simple interpretation of the observed systematic decrease of shear resistance with increasing  $n$  is that, in the vicinal limit of large  $n$ , the resistance should approach that of the  $(\bar{1}10)$  plane ( $n=1, m=0$ ) or, equivalently, of the  $(0\bar{1}\bar{1})$  plane ( $n=0, m=1$ ). Approaching this limit, the resistance can be thought of as a combination of the resistance associated with the  $(\bar{1}10)$  “terrace” and the resistance associated with the  $(0\bar{1}\bar{1})$  step. Assuming that the resistance per unit area of the terrace is  $\sigma_{\text{terr}}$  and that per unit area of the step is  $\sigma_{\text{step}}$ , the resistance per unit area of vicinal plane  $n$  can be written as

$$\sigma_n = \frac{n\sigma_{\text{terr}} + \sigma_{\text{step}}}{\sqrt{n^2 + n + 1}}. \tag{3}$$

Assuming further that  $\sigma_{\text{terr}} = \sigma_{\text{step}}$ , the above formula reproduces the computed resistances remarkably well for the whole vicinal family of planes. For the vicinal subset of planes  $(n, 1)$  considered here, the spacing between the planes is a simple function of  $n$  making it possible to rewrite the above expression in terms of the plane

spacing  $d$ :

$$\frac{\sigma(d)}{\sigma(0)} = \frac{1}{2} \left[ \frac{d}{d_0} + \sqrt{4 - 3 \left( \frac{d}{d_0} \right)^2} \right], \quad (4)$$

where  $\sigma_0$  and  $d_0$  are the resistance and the interplanar spacing for the  $\{110\}$  planes. Somewhat surprisingly, the above two formulae are accurate even for the  $(\bar{1}2\bar{1})$  plane that is in the middle between the terrace and the step planes. This is suggestive that, perhaps, the resistance in a general plane  $(n, m)$  can be approximated by a straightforward extension

$$\sigma_{\text{th}}(n, m) = \sigma_{\text{th}}(1, 0) \frac{n + m}{\sqrt{n^2 + m^2 + mn}}, \quad (5)$$

where  $\sigma_{\text{th}}(1, 0) = \sigma_{\text{th}}(1, \infty) = \sigma_{110}$  is the resistance for the terrace ( $n=1, m=0$ ) and step ( $n=0, m=1$ ) planes. Even if for general values of  $n$  and  $m$  there is no longer any simple relation between  $n$  and  $m$  and the interplanar spacing  $d$ , the above resistance can be re-written instead as a function of angle  $\theta = \arctan[\sqrt{3}m/(2n+m)]$  between the terrace plane  $(\bar{1}10)$  and plane  $(n, m)$ :

$$\sigma(\theta) = \sigma_{110} \left[ \cos(\theta) + \frac{1}{\sqrt{3}} \sin(\theta) \right] \quad (6)$$

$$0 \leq \theta \leq 60^\circ.$$

Plotted as a function of angle  $\theta$ , the predictions based on equation (6) agree very well with the computed resistance in the whole range of angles (figure 3). Thus, for the model of bcc molybdenum examined here, it is not the plane spacing  $d$  but the plane angle  $\theta$  that is an accurate predictor of the ideal shear resistance.

It is possible to further rationalize equations (5) and (6) through a bond counting argument. It is easy to see, by direct inspection, that for any rational plane  $(n, m)$ , the number of nearest neighbour bonds distorted by the shear displacement per one repeat distance along the PEV is  $(n+m)$  times larger than the number of bonds per repeat distance distorted by shearing along the terrace plane  $\sigma_{110}$ . To obtain the needed resistance it is necessary to divide  $(n+m)$  by the length of the repeat distance along the PEV, i.e. by  $\sqrt{n^2 + m^2 + mn}$ . Another interpretation of the same function can be given in terms of the effective potential describing the interaction between the infinite rows of atoms spanning the crystal lattice along  $[111]$  direction, an ‘‘inter-row’’ potential [13]. Defined per unit length of the atomic row and allowing no displacements in the directions perpendicular to  $[111]$ , this potential is a function of relative position of two rows along the  $[111]$  axis. Assuming that the inter-row potential is a pair potential and acts only between the nearest neighbour rows and taking into account the initial displacements  $x_0$  between the pairs of atoms rows ( $x_0 = 0, b/3, \text{ or } 2/3b$ , depending on the pair), the energy per unit area of any plane  $(n, m)$  can be written as an appropriate sum over the inter-row potentials immediately leading to equations (5) and (6).

Strictly speaking, a relationship of this kind should be accurate only for crystals in which the interatomic interactions are well described by extremely short-ranged

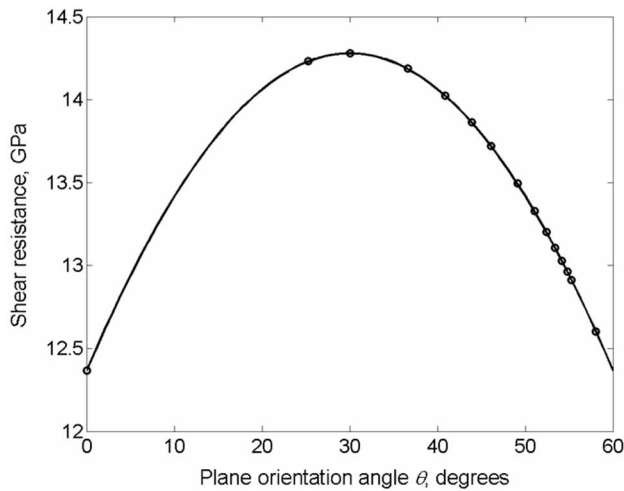


Figure 3. The ideal shear resistance (circles) computed using method 1 for planes in the  $\langle 111 \rangle$  zone of BCC molybdenum plotted as a function of the plane orientation angle  $\theta$  counted anticlockwise from the  $(\bar{1}10)$  terrace plane. The solid curve is equation (5) in the same coordinates.

pair potentials. However, even though small but discernible differences between equation (6) and the resistances computed atomistically do exist, the formula is rather accurate for the Finnis–Sinclair model of molybdenum which is neither a pair potential nor particularly short-ranged [11]. (In particular, for all planes but  $\{110\}$ , the resistance to shear in one direction along the Burgers vector  $\frac{1}{2}[111]$  is different from the resistance computed for shearing in the opposite direction. Such differences manifest the so-called “twinning–anti-twinning” asymmetry [14]. This asymmetry in the resistances computed with methods 1 and 2 is rather small for the FS model considered here.) Still, it is probably too optimistic to regard equations (5) and (6) as much more than interpolation functions inspired by a bond counting argument. Their applicability to the resistances computed by methods 2 and 3 is even more questionable. But even there, given that the computed resistances are very close to those obtained by method 1 (rigid-block-sliding), equations (5) and (6) can be used for reasonably accurate interpolations.

#### 4. Results and discussion – fcc crystal

In fcc materials, the shear resistance is usually lowest for the low energy shear paths along  $\langle 112 \rangle$  directions in the  $\{111\}$  planes: related to this is the notorious tendency of perfect  $\frac{1}{2}\langle 110 \rangle$  dislocations to dissociate into two  $\frac{1}{2}\langle 112 \rangle$  Shockley partials separated by a planar fault in a  $\{111\}$  plane. Here, we are primarily interested in finding possible connections between lattice symmetry and geometry and shear resistances in fcc materials. For that reason, rather than focusing on the  $\langle 112 \rangle\{111\}$  shear path we intend to examine the resistance to shear along multiple planes in the

zone defined by the  $\frac{1}{2}(110)$  Burgers vector of the perfect dislocations. For the reader's reference, the resistance to shear along  $\langle 112 \rangle$  directions computed with the Ercolessi–Adams EAM potential for aluminium was 1.90 GPa (method 1) and 1.92 GPa (method 2).

Similar to the bcc case discussed in the preceding section, the computed shear resistances in fcc aluminium do not reveal any systematic relationship to the spacing between the shear planes. However, when plotted as a function of plane orientation (figure 4), the data shows systematic variations with well defined maxima for the  $\{001\}$  and  $\{110\}$  planes and a cusp-shaped minimum for the  $\{111\}$  plane. At first we

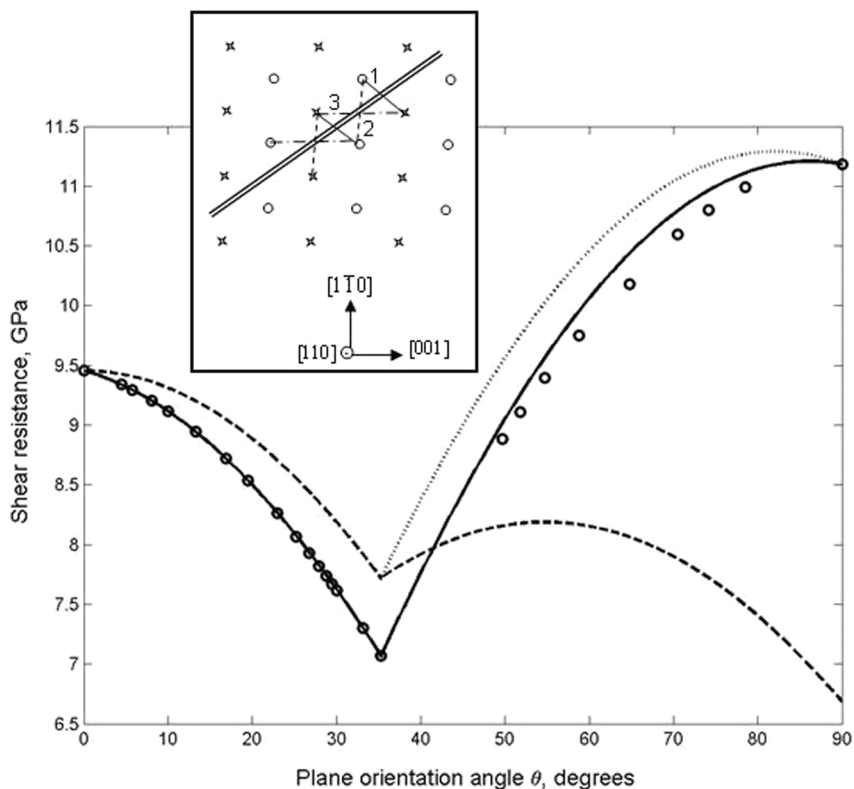


Figure 4. Shear resistances computed by method 1 (circles) for planes of varying orientation. The dashed line is the one-parameter fit, the dotted line is the two-parameter fit (the fit on the left of the cusp remains the same as in the one parameter fit), and the solid line is the three-parameter fit (see text). The inset shows three types of bonds distorted by shearing the crystal in  $[110]$   $z$ -direction (into the plane) along one of its crystallographic planes shown by a double line. The open circles label the atoms (and atomic rows) that are in the picture plane ( $z=0$ ) and the crosses label the atoms (and atomic rows) that are offset from the picture plane by half of the repeat distance ( $z=-b/2$ ). The thin solid lines crossing the plane are type 1 bonds connecting the nearest neighbour atom pairs that move closer towards each other during shearing. The thin dashed lines are type 2 bonds connecting the nearest neighbours that move apart during shearing. The dash-dotted lines are type 3 bonds connecting the second nearest neighbours that change their relative positions during shearing.



used the same bond counting procedure as in section 3 and scaled the curve to match the resistance for the  $\{110\}$  plane ( $\theta = 0^\circ$ ). The resulting curve (dashed on the figure) reproduces the existence of a cusp for the  $\{111\}$  plane ( $\theta = 35.26^\circ$ ) but otherwise does not fit the computed data very well. By inspecting the fcc lattice geometry, one can readily observe that, among the nearest neighbour bonds that are distorted by shearing along the  $\langle 110 \rangle$  direction, there are actually two different types. Bonds of type 1 become shorter during shearing whereas bonds of type 2 become longer (see the inset in figure 4). It is then reasonable to assign different contributions to the bonds of two different types and count their numbers (per unit area) separately for a given plane orientation. The interpolation function derived from such counting contains two scaling parameters that were then chosen to match the data computed for two special plane orientations:  $\theta = 0^\circ$  ( $\langle 110 \rangle$  plane) and  $\theta = 90^\circ$  ( $\langle 001 \rangle$  plane). The resulting fit (dotted line on the figure) is considerably closer but fails to match the resistance computed for the cusp orientation ( $\langle 111 \rangle$  plane). To further improve the fit, it seems necessary to introduce one more scaling parameter. In keeping with the bond counting argument we relied on so far, let us assign a specific resistance value to every second nearest neighbour bond (type 3) and count the number of such bonds per unit area distorted during the shearing. By separately counting the bonds of all three distinct types and requiring that the resulting interpolation functions match the data points obtained for three special planes, we arrive at the following function

$$\sigma(\theta) = \sigma_{110} \cos \theta + \left( \sqrt{3}\sigma_{111} - \sqrt{2}\sigma_{110} \right) \sin \theta \quad (7)$$

for angles  $0^\circ \leq \theta \leq 35.26^\circ$  and

$$\sigma(\theta) = \sigma_{001} \sin \theta + \frac{1}{\sqrt{2}} \left( \sqrt{3}\sigma_{111} - \sigma_{001} \right) \cos \theta \quad (8)$$

for angles  $35.26^\circ \leq \theta \leq 90^\circ$ . The resistance for all other plane orientations can be obtained by fcc crystal symmetries.

The resulting three-parameter interpolation function closely matches the computed shear resistances in the whole range of plane orientation (solid line on the figure), although the fit on the right of the cusp is less than perfect. Rather than trying to improve the fit still further, it may be more interesting to examine the reasons for the remaining discrepancies. As was already mentioned, the bond counting arguments presented so far can be expected to be accurate only for extremely short-ranged pair potentials. As was the case in the preceding section, the EAM potential used here is neither short range nor pair-wise. To find out which of the two factors, the extended range or the many-body character of the EAM potential, is responsible for the remaining discrepancies, we performed an identical series of calculations using a 6-12 Lennard-Jones (LJ) pair potential with a relatively long cut-off radius.

The results are plotted on figure 5. The general shape of the angular dependence is very similar to that obtained for the EAM potential. It turns out that a nearly perfect fit of this data (the solid line on the figure) can be obtained with just two

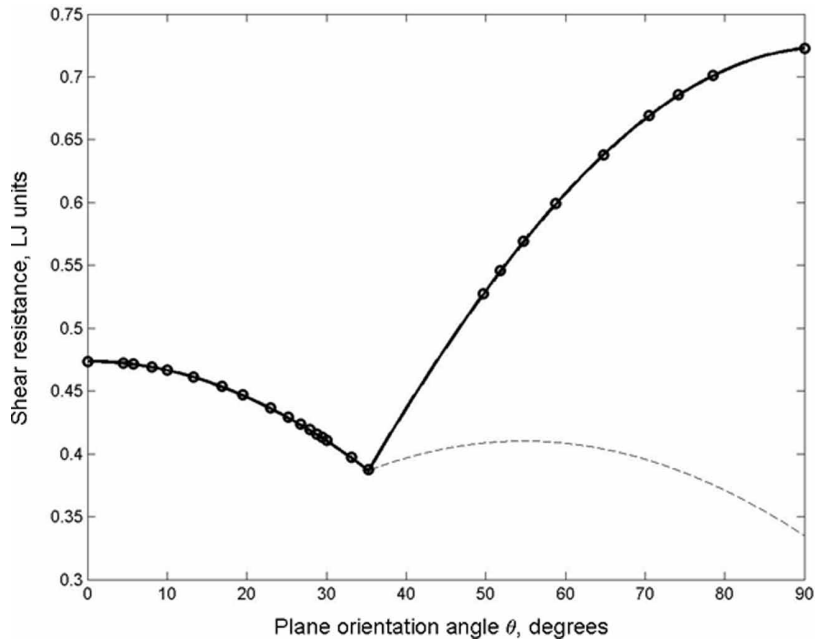


Figure 5. Shear resistances computed by method 1 (circles) for planes of varying orientation using the Lennard-Jones pair potential. The dashed line is a one-parameter fit assuming that bonds of types 1 and 2 make equal contributions to the shear resistance. The solid line is the two-parameter fit (see text).

scaling parameters computed by requiring the interpolation function to match the data at the ends of the angular interval  $0^\circ \leq \theta \leq 90^\circ$ . The resulting function is

$$\sigma(\theta) = \sigma_{110} \cos \theta \quad (9)$$

for angles  $0^\circ \leq \theta \leq 35.26^\circ$  and

$$\sigma(\theta) = \sigma_{001} \sin \theta + \left( \sigma_{110} - \frac{\sigma_{001}}{\sqrt{2}} \right) \cos \theta \quad (10)$$

for angles  $35.26^\circ \leq \theta \leq 90^\circ$ . Given that the LJ potential used in calculations was relatively long-ranged ( $r_{\text{cut}} > 2a$ ), we are left to “blame” the many-body character of the EAM potential for the discrepancies observed in figure 4.

The shear resistances computed for planes in the  $\langle 110 \rangle$  zone using method 2 with the same EAM potential are shown in figure 6. The effect of vertical relaxation observed for the EAM model of fcc aluminium is considerably larger than in the bcc system examined earlier. For the particularly resistant  $\{001\}$  plane, the relaxation brings the resistance down by more than a factor of two. Nevertheless, similar angular functions can be used to fit the relaxed data with an acceptable accuracy by matching to the computed values of shear resistance for three special planes,  $\{110\}$ ,  $\{111\}$  and  $\{001\}$ .

It has been argued in the literature that GSF surfaces computed by allowing the vertical relaxation are more representative measures of shear resistance than the

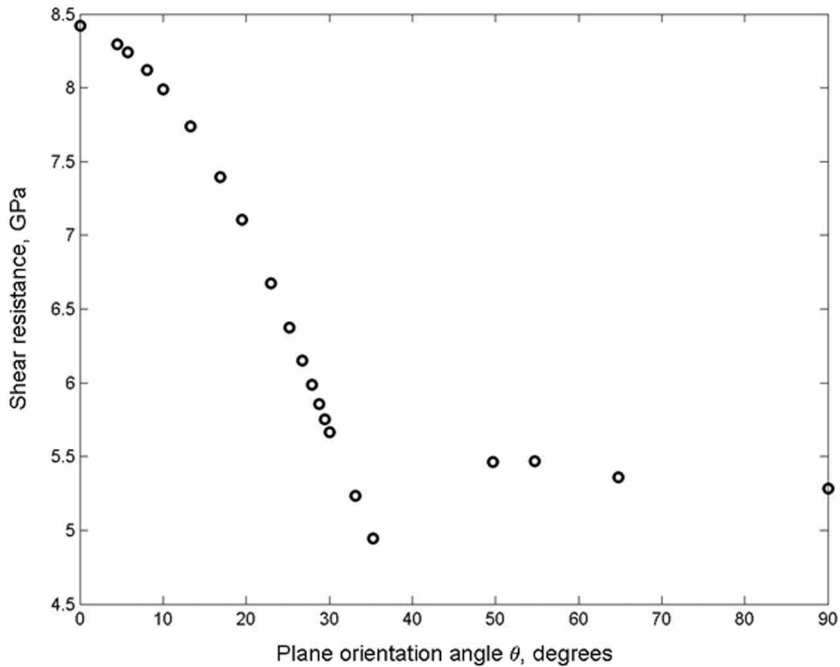


Figure 6. Shear resistances computed by method 2 for planes of varying orientation using the EAM potential for aluminium.

unrelaxed GSFs. We would like to assert that neither relaxed nor unrelaxed GSFs offer an entirely accurate description of the energetics of interplanar shear. A better description was proposed by Bozzolo *et al.* [15] who suggested to extend the GSF concept to include an additional, third variable describing the spacing between two atomic planes. Such a three-dimensional GSF can serve as an accurate input for a Peierls–Nabarro calculation allowing for the additional degree of freedom during nucleation and motion of dislocations or shear faults. As was shown by Bulatov and Kaxiras [16] and Xu *et al.* [17], such an extension leads to a more accurate description of dislocations in silicon than either unrelaxed or fully relaxed GSF surface can provide.

## 5. Summary

The observations reported and analyzed in this contribution show that the literal interpretation of Frenkel’s equation, equation (1), as  $\sim 1/d$  scaling function for the ideal shear resistance is a misconception. In fairness, in his classic paper [2] Frenkel arrived at equation (1) by considering a plane in the crystal lattice: nowhere did he suggest that shear resistances along different planes in the same crystal scale as  $\sim 1/d$ . It is rather likely that the now common interpretation developed at a later time, possibly reinforced by the empirical observations of slip along the widely spaced

planes in single crystals. Here we report that the well known  $\{110\}$  planes in bcc and  $\{111\}$  planes in fcc crystals are indeed the planes of minimal shear resistance, irrespective of the magnitude of the interplanar spacing. Based on bond counting arguments, we present scaling equations that provide adequate descriptions of the ideal resistance as functions of plane orientation. We would like to emphasize that the particular forms of interpolation functions presented here are fixed by symmetry and geometry of bcc and fcc lattices, respectively. In our approach, the differences between two crystals with the same crystal lattice are subsumed in the material-specific scaling parameters.

It remains to be seen if bond counting or some other considerations can lead to still more accurate interpolation functions. In particular, the discrepancies remaining in figure 4 require further attention. Another important issue we are currently addressing is if and how the observed angular dependences of the ideal shear resistance affect the properties of dislocations on various planes. For fcc and other similar materials, the  $\{111\}$  planes are selected for glide by the planar dissociation of perfect dislocations into Shockley partials. In other materials, e.g. bcc metals, multiple planes can be involved in the dislocation glide. An even more interesting behaviour can be found in ordered alloys with very large unit cells [18]. Given the variability and complexity of their crystal structures, it is highly desirable to have a means to relate, at least qualitatively, the symmetry and geometry of their crystal lattices to the resulting shear strength. We hope that the simple study presented in this paper can serve as a useful starting point in this direction.

### Acknowledgements

This work was performed under the auspices of the US Department of Energy by the University of California, Lawrence Livermore National Laboratory under Contract No. W-7405-Eng-48. This work was supported by the Office of Basic Energy Sciences US Department of Energy and the NNSA ASC Program. VVB wishes to express his gratitude to W. G. Wolfer for fruitful discussions, encouragement and help. The authors also wish to thank B. Sadigh and G. H. Gilmer for their interest and useful suggestions.

### References

- [1] M.S. Duesbery and G.Y. Richardson, *Crit. Rev. Solid St. Mater. Sci.* **17** 1 (1991).
- [2] J. Frenkel, *Z. Phys* **37** 572 (1926).
- [3] J.P. Hirth and J. Lothe, *Theory of Dislocations* (Wiley, New York, 1982), p. 6.
- [4] R.E. Peierls, *Proc. Phys. Soc.* **52** 23 (1940).
- [5] F.R.N. Nabarro, *Proc. Phys. Soc.* **59** 256 (1947).
- [6] J.A. Moriarty, J.F. Belak, R.E. Rudd, *et al.*, *J. Phys. Condensed Matter* **14** 2825 (2002).
- [7] A.T. Paxton, P. Gumbsch and M. Methfessel, *Phil. Mag. Lett.* **63** 267 (1991).
- [8] E. Kaxiras and M.S. Duesbery, *Phys. Rev. Lett.* **70** 3752 (1993).
- [9] V. Vitek, *Phil. Mag.* **18** 773 (1968).

- [10] B. Joos, Q. Ren and M.S. Duesbery, *Phys. Rev. B* **50** 5890 (1994).
- [11] M.W. Finnis and J.E. Sinclair, *Phil. Mag. A* **50** 45 (1984).
- [12] F. Ercolessi and J.B. Adams, *Europhys. Lett.* **26** 583 (1994).
- [13] H. Suzuki, in *Dislocation Dynamics*, edited by A.H. Resenfield, *et al.* (McGraw Hill, New York, 1967).
- [14] F.S. Duesbery and V. Vitek, *Acta Mater.* **46** 1481 (1998).
- [15] G. Bozzolo, J. Ferrante and J.R. Smith, *Scripta Metall.* **25** 1927 (1991).
- [16] V.V. Bulatov and E. Kaxiras, *Phys. Rev. Lett.* **78** 4221 (1997).
- [17] G. Xu, A.S. Argon and M. Ortiz, *Phil. Mag. A* **75** 341 (1997).
- [18] M. Heggen and M. Feuerbacher, *Mater. Sci. Engng* **400** 89 (2005).